Check for updates

Experimental study and a physical model on the geomorphic response mechanisms of meandering rivers under progressive sediment reduction

Zhanchao Zhao[1,2,3], Shiming Yao[4], Enhui Jiang[1,2,3]* and Bo Qu[2,3]

[1]College of Water Conservancy and Hydropower Engineering, Hohai University, Nanjing, Jiangsu, China, [2]Yellow River Institute of Hydraulic Research of Yellow River Conservancy Commission, Zhengzhou, Henan, China, [3]Key Laboratory of Lower Yellow River Channel and Estuary Regulation, MWR, Zhengzhou, Henan, China, [4]Yangtze River Scientific Research Institute, Wuhan, Hubei, China

As influenced by human activities, including high dam construction, soil and water conservation, and sand mining in the upper reaches of rivers, the amount of sediment entering the lower reaches of the river decreases significantly. Human activities disturb the natural balance between river evolution and water as well as sediment movement and induce new characteristics of river evolution. After the construction and operation of the Danjiangkou Reservoir and the Three Gorges Reservoir of the Yangtze River (China), different degrees of bend bypassing and shoal cutting in the bends downstream of the dams are observed. The reason for this interrelation has not been explained sufficiently. Based on the analysis of prototype observation data and physical model experiments, we have investigated the evolution mechanism of different topographic types of meandering rivers under the condition of decreasing sediment inflow. The data generated by our model experiment document that the sediment concentration of the convex bank flow with a large degree of curvature of the bend is lower than that of the concave bank flow for a reduction of the sediment concentration from 100% to 0%. Moreover, the convex bank of the bend gradually collapses and retreats, whereas the main channel of the river gradually swings, with a swing range of 0−800 m, toward the convex bank. This phenomenon becomes more significant with progressive reduction of the sediment inflow. Combined with theoretical analysis, we interpret that the drastic reduction in the amount of sand that has destroyed the relative natural balance of sediment transport in the riverbanks and river channels in the meandering river section is the main reason for the occurrence of bypassing and shoal cutting in the meandering river section of plain alluvial rivers. Especially during the mid-to high-water period, the capacity of sediment transport in the mainstream belt exceeds the sediment concentration in the water body significantly and is coupled with the change of the runoff process caused by the regulation of the reservoir operation. As a consequence, the river beach is constantly scouring and developing. The evolution is generally characterized by bend bypassing and shoal cutting. The results of our study

can be transposed to other alluvial plain rivers and may constitute valuable reference data.

1 Introduction

The meandering river is one of the most common types of natural rivers. Its evolution is closely controlled by the incoming flow and sediment conditions, river boundary conditions, and riverbed composition. The evolution of natural alluvial meandering rivers generally follows the evolution characteristics of concave bank scour and convex bank siltation or bend bypassing and shoal cutting and cutting and straightening after excessive bending. The evolution of the meandering river affects the flood control, navigation, protection, and utilization of water and soil resources along the shoreline. Therefore, to better control the evolution of meandering rivers, river regulation has been conducted to meet various needs. In recent years, the incoming flow and sediment conditions as well as river boundary conditions have been changed due to the aggravation of human activities that has a major impact on the evolution of meandering rivers. Two main methods for the study of meandering rivers exist 1. prototype observation and analysis and 2. model experiments. In recent years, many studies have focused on the downstream meandering river after the construction of the barrage.

1.1 Prototype observation and analysis

The primary task of studying the evolution characteristics of the meandering river is to observe and analyze the natural river. The prototype observation data of the Mississippi River in the United States (Fisk, 1945; Furbish, 1991; Harmar and Clifford, 2010) and the Bollin River in England (Luchi et al., 2010) have shown the phenomenon of bend bypassing and shoal cutting in the meandering river. The characteristics of bend bypassing and shoal cutting vary with different degrees of curvature. Under the condition of natural sediment inflow, the sediment transport in a meandering river is in relative equilibrium. The maximum bed load transport zone follows the outward movement of the maximum boundary shear force, and the maximum sediment transport is close to the center line of the river channel. The main factors affecting the lateral flow and sediment movement are the river channel topography and the transverse velocity distribution of the meandering river channel, as documented in the Muddy Creek River in the United States (Dietrich and Smith, 1984). Based on the channel sediment supply mechanism and combined with the channel satellite observation map, the variation characteristics

of the floodplain shear force of the meandering river and the evolution law of the floodplain of the meandering river under different types of sediment supply and transport mechanisms were analyzed (Constantine et al., 2014). Plants existing in the meandering channel have an impact on the bank structure, the floodplain flow, and sediment transport and can change the topography of the meandering channel accordingly. The evolution characteristics of the meandering channel in the Tagliamento River (Italy) have been analyzed under the influence of plants by using lidar observation technology and prototype measured data (Zen et al., 2017). Based on satellite observation data, the change data of curved river width are counted, and a model is constructed that can simulate the evolution of river banks and determine the model parameters. The model can be used to calculate the long-term evolution characteristics of meandering rivers and has been applied to a section of the Ucayali River (Peru) (Sergio and Stefano, 2019). Arnez et al. (2021) studied through remote sensing analysis and field investigation, using 30 years of observation data, the planform evolution and riverbed topography of the Ichilo River (Bolivia), a small river located in the upper foreland Amazon basin. Their findings show that cutoffs, climate, and human activities are the main factors that control the meander migration rates in the Ichilo River. With the construction of a river barrage project, the river flow and sediment conditions have changed, and the sediment transport in the meandering river follows a new principle. Hence, continued prototype monitoring is required.

1.2 Model experiment

Numerical simulation and generalized model experiments are commonly used to study the characteristics of flow and sediment movement in different meandering channels. The model experiment of large-scale meandering reaches can explain the flow characteristics, sediment transport characteristics, bed terrain change characteristics, and the influence of the curvature on the plane shape of the sharp meandering reach with a large degree of curvature (Whiting and Dietrich, 1993). The two-dimensional flow model is combined with the average topographic depth model of the riverbed and the bank erosion model of the meandering channel to simulate the riverbed boundary and riverbed deformation of the meandering channel. The model is corroborated by a flume experiment and measured data of the

natural meandering channel and provides the possibility to simulate the shear stress at the boundary of meandering channels. However, the model is inapplicable for the accurate simulation of quantifying the change characteristics of the meandering channel (Darby et al., 2002). Kassem and Chaudhry (2002) developed a two-dimensional model to study the time variation of the riverbed deformation in a meandering river. Comparing the data with the experimental results of 140° angle and 180° angle meandering channel flumes shows that the model is suitable for unsteady flow and meandering rivers with irregular boundaries. The long-term evolution principle of the channel has been analyzed from the perspective of considering the dynamic process of different forms of the meandering channel, and the shape and curvature of the meandering channel are recognized as the main factors that affect the morphological dynamic process of the evolution of the meandering channel (Frascati and Lanzoni, 2009). Flume experiments have been conducted to analyze the conditions that are necessary to maintain meandering channels in coarse-bedded rivers, and the experimental results show that the characteristics of the incoming sediment are the main factors that affect the topographic changes of curved river channels (Braudrick et al., 2009). The flume experiments with large curvatures have been used to analyze the flow movement characteristics of a large amplitude meandering bend, and the studies show that the counter-rotating circulation cell only occurs in the case of a "small" width-to-depth ratio (Donatella and Mafalda, 2011). Using a physical model, Güneralp and Rhoads (2011) studied the impact of the erosivity of floodplain flow on the evolution of plane riverbed in meandering channels and recognized that the complexity of plane riverbed shape depends on the spatial scale difference and random variability of erosion. Xu and Bai (2013) used the generalized sinusoidal derivative curve to conduct an experimental study on the meandering flume and analyzed the characteristics of riverbed deformation in combination with the characteristics of flow and sediment movement in the meandering channel with different degrees of curvature. He proposed that the curvature of the meandering channel and the boundary conditions of the channel itself affect the stability of channel deformation. The instability of riverbed deformation increases with the increasing degree of the channel curvature (Xu and Bai, 2013). Keshavarzi et al. (2016), Amirhossein et al. (2020), and Lindroth et al. (2020) have used physical model experiments to investigate the impact of the type and distribution of river vegetation on the meandering river. Their studies show that the characteristics of the vegetation in the river channel have an impact on the cross-sectional flow velocity, the sediment distribution, and the riverbed shear stress of the curved river channel; thus, they strongly affect the topographic changes of the riverbed of the curved river channel. In future river training projects, the impact of the vegetation can be used to control the evolution of the meandering river.

1.3 Study on the meandering rivers downstream of the barrage

The empirical formula of the ideal meandering shape in the middle and lower reaches of the Han River in China has been established according to the morphological characteristics of 32 typical meandering channels in the middle and lower reaches of the Han River (Zhang et al., 2007). The flow conditions have been considered in the study as an important factor causing the phenomenon of bend bypassing and shoal cutting in the middle and lower reaches of the Han River. Qin et al. (2009) have established a formula for the meandering radius of the dynamic axis of flow suitable for the Jingjiang River reach in China and have analyzed the relationship between the change of the meandering radius of the dynamic axis of flow and the phenomenon of bend bypassing and shoal cutting. After the construction of the barrage in the river, the oscillation characteristics of the dynamic axis of flow in the downstream reach will change (Hooke and Yorke, 2011).

After the construction of the Three Gorges Reservoir in the Yangtze River, the sediment inflow in the lower reaches of the reservoir has gradually decreased, and the evolution characteristics of bend bypassing and shoal cutting have appeared in the lower reaches of the meandering river. After the operation of the Three Gorges reservoir, the flow, sediment, and river regime downstream of the dam have significantly changed, and the evolution characteristics of the Jingjiang River reach of the Yangtze River have been adjusted. The changes in flow and sediment conditions as well as the river boundary conditions are the main factors for the river channel adjustment of the Jingjiang river reach (Sixuan et al., 2018). The change of the riverbed and the geological conditions have also been considered to be the causes of bend bypassing and shoal cutting in the meandering channel of the Jingjiang River (Li et al., 2013). After the construction and operation of the Three Gorges reservoir, the clear water has been discharged, the mainstream line and thalweg of the meandering river course have shifted strongly, and the cross-section shape of the river course changes from V shape to W shape (Ruan, 2016). The change in the flow process, the change of time distribution of the position of the dynamic axis of flow, and the reduction of sediment inflow are the main causes of "convex scouring and concave silting" in the meandering channel of the lower Jingjiang River (Zhu et al., 2017). The observations indicate that the driving factors of the meandering channel evolution are the changes of upstream river regime, the river boundary conditions, and incoming flow and sediment conditions (Fan et al., 2017).

Striking progress has been made in previous studies in the understanding of the overall evolution characteristics and channel characteristics of meandering channels, which provides a basis for further studies on meandering channels. Rivers are complex systems. Flow and sediment movement, as well as the geomorphic change caused by flow and sediment

TABLE 1 Change of sediment transport in the Yangtze River and the Yellow River (China).

	Tongguan hydrological station (Yellow River)			
Particular year	1980–1989	1990–1999	2000–2009	2010–2016
Average annual sediment discharge (10^8t)	7.803	7.90	3.12	1.57
	Jianli hydrological station (Yangtze River)			
Particular year	1981–1991	1992–2002	2003–2007	2008–2017
Average annual sediment discharge (10^8t)	4.68	3.44	0.93	0.33

movement, may induce large-scale environmental problems. The analysis of prototype observation data is an effective research method, which can be used to analyze the evolution characteristics and influencing factors of the meandering river from a large-scale perspective. However, due to prototype limitations, observation of large-scale rivers, especially sediment movement, is difficult, and the internal processes of the geomorphic change of the meandering river still need further exploration. The physical model clearly and intuitively reflects the characteristics of natural river geomorphic changes and overcomes the limitations of sediment and geomorphic monitoring. The physical model method is required to corroborate the studies on the internal mechanisms of river flow and sediment movement and river geomorphic change. Based on the theoretical analysis of prototype observation data, the physical model is used to simulate the natural river section, control the sediment inflow, and study the influence mechanism of sediment inflow on the geomorphic deformation of the meandering river. In the present study, we focus on analyzing the coupling mechanism between the sediment concentration of the flow and the topographic change characteristics of the curved channel to decipher the riverbed evolution characteristics of the meandering river downstream of the barrage. Our findings will provide a profound reference for river regulation, presumably applicable to the study of other plain alluvial rivers in the world.

2 Prototype analysis

2.1 Variation of flow and sediment conditions

The measured data of hydrology stations in the middle reaches of the Yangtze River and the Yellow River in China are analyzed (Table 1). In recent years, a dramatic decrease in the sediment discharge in the river channels has been detected, with a reduction in the Yangtze River and the Yellow River of about 80–90% since 2010. Human activities, including the construction of high dams with large reservoirs, soil and water conservation, and sand mining, are the main causes of the sediment decrease. The sediment discharge has decreased gradually. The composition of the suspended sediment and bed material in the river channel and the sediment transport process have changed. Moreover, the exchange of sediment carried by flow and bed material shows new characteristics, and the river landform exhibits a new pattern.

The flow and sediment data of the Shashi hydrological station on the Yangtze River in China are selected for a detailed analysis (Table 2). The selected time span ranges from 1981 to 2017, which is divided into four periods and two periods, respectively (the four periods are divided according to the operation of the Three Gorges reservoir, and the two periods represent the time before and after the operation of the Three Gorges reservoir). The Shashi hydrological station is located upstream of the continuous meandering river section (Tiaoguan-Laijiapu reach and Xiongjiazhou-Chenglingji reach) and is selected for the study (Figure 1), and it is located about 180 km away from the upstream Three Gorges dam. Water storage and operation of the Three Gorges Reservoir started in 2003. The water inflow of the Shashi hydrological station has not changed significantly before and after the operation of the reservoir, but the sediment load has decreased significantly after the operation of the reservoir. After the operation of the reservoir (2003–2017), the average annual sediment load was reduced by 86.70% when compared with the data prior to operation (1981–2002). The distribution trend of the average daily flow in the four periods remained nearly constant (Figure 2). The highest flow level occurred from June to October, whereas from November to May, the flow level is low to moderate. After the operation of the Three Gorges reservoir, the reservoir has played a major role in the regulation of the discharge flow. Flow levels <5,000 m³/s and >25,000 m³/s have decreased, and flow levels >5,000 m³/s and <25,000 m³/s have increased. Moreover, the incoming flow process has become progressively flattened. After the operation of the Three Gorges reservoir, the daily average sediment concentration has decreased significantly.

2.2 Topographic change

We have selected prototype geomorphological observation data of two typical meandering reaches of the Yangtze River and twelve observation sections and three observation years for the

TABLE 2 Variation of annual runoff and annual sediment discharge of the Shashi hydrological station.

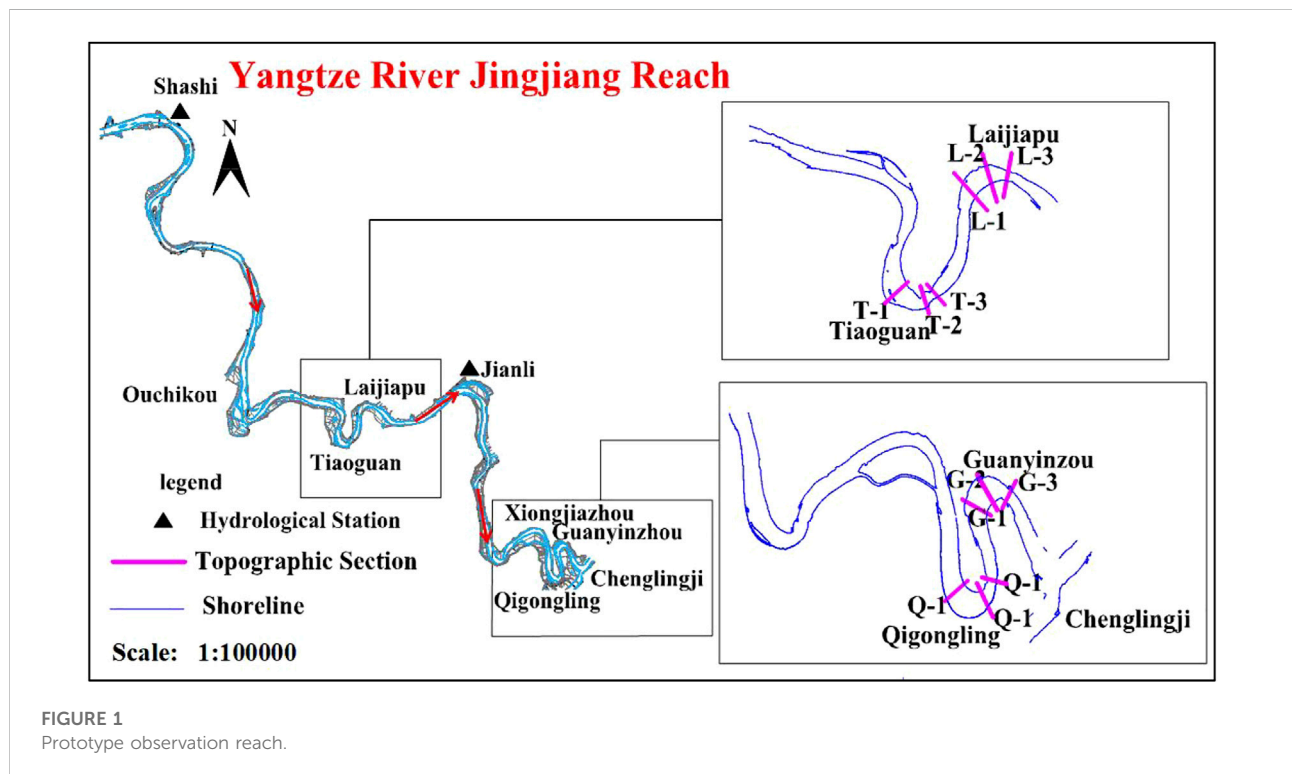| Time span		1981–1991	1992–2002	1981–2002	2003–2007	2008–2017	2003–2017
Shashi hydrological station (Yangtze River)	Average annual runoff (10^8m^3)	4,080	3,994	4,037	3,720	3,836	3,797
	Average annual sediment transport (10^8t)	4.68	3.44	4.06	0.93	0.33	0.54

FIGURE 1
Prototype observation reach.

analysis (Figure 1). The observed section is located in the middle and lower reaches of the Yangtze River, including meandering reaches with different radii of curvature. Most sections on the right bank of the river are hilly terraces with strong anti-scouring capacity. The left bank of the river is an alluvial plain. A double-layer structure of recent river sediments dominates the riverbank. It is composed of a lower sand layer and an upper cohesive soil layer with poor anti-scouring capacity. The riverbed is composed of medium-to fine-grained sand with a median particle size of about 0.165 mm. The pebble layer is deeply buried below the bed surface.

We have selected the T-1, Q-1, and G-1 river sections for a detailed analysis (Figure 3). The three sections are located in the middle and upper positions of the meandering reach. The convex bank and edge beach at the three cross sections are scoured, and the riverbed elevation decreases. The concave bank is silted and the riverbed elevation increases. The nearshore central bar is formed on the concave bank side, and the river section changes from V shape to W shape. This phenomenon is termed bend bypassing and shoal cutting, which is different from the convex bank silting and concave bank scouring of the ordinary meandering channel that was described in previous studies. According to the change of the channel plane shape between 2002 and 2016 (Figure 4), the river channel was mainly scoured. The specific manifestations are beach scouring and deep channel siltation. The main river channel is shifted from the concave bank to the convex bank. The transition section of the bend is dominated by scouring, and at the bend position, it is mainly characterized by convex bank scouring and concave bank silting. The scouring and silting changes at sections T-1 and G-1 are relatively severe, and the maximum scouring depth and maximum siltation thickness at the two positions are 13 m and 18 m (T-1), and 29 m and 19 m (G-1), respectively.
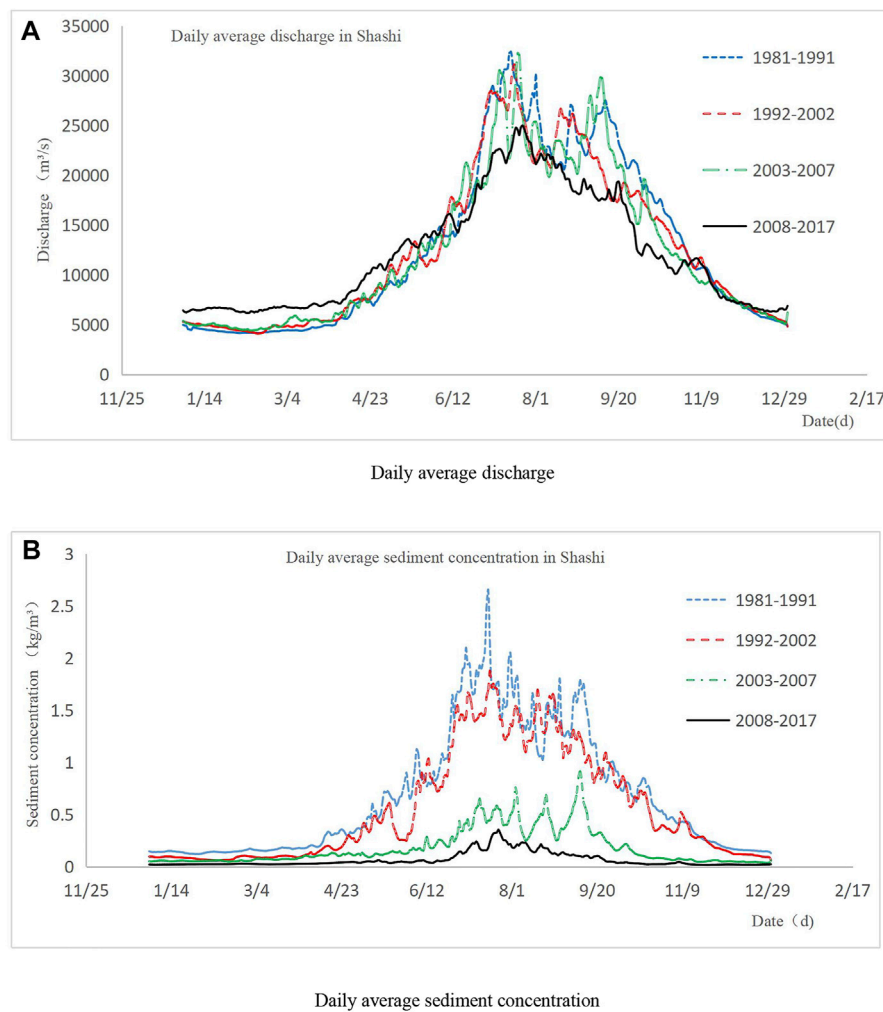
FIGURE 2
Variation of daily average discharge and daily average sediment concentration at the Shashi hydrological station.

2.3 Analysis of theoretical results

The change of the river landform is the mutual adaptation and development of the riverbed and the flow and sediment conditions. The riverbed will be adjusted to the changes in the flow and sediment conditions. After the impoundment and operation of the Three Gorges reservoir, no significant change in the total amount of water coming from the lower reaches occurred, but the flow process changed significantly. The increase of the occurrence time of medium flow level (5,000–25,000 m ^{3}/s) was the main modification. After the operation of the reservoir, the total amount of sediment inflow decreased significantly, and the sediment concentration dropped gradually during sediment inflow. The sediment concentration of flow cannot satisfy the sediment carrying capacity of the flow. In order to satisfy the sediment carrying capacity of flow, the flow will scour the riverbed. Therefore, the convex bank of the meandering river is subject to cumulative scouring. As a consequence, the edge beach of the convex bank continues to collapse, and the riverbed elevation decreases. Finally, the phenomenon of bend bypassing and shoal cutting is initiated. According to the observation and analysis of the prototype data, the causes of this phenomenon are the reduction of sediment from the river and the change in the runoff process caused by the operation and regulation of the reservoir. The prototype data observation allows analyzing the causes for the change of the meandering channel landform under the condition of sediment reduction from a macro perspective. However, as the observation of large-scale rivers is difficult, it remains problematic to obtain the cross-sectional distribution of sediment, the velocity, and the change of topography under different flow levels from natural rivers. Therefore, it is necessary to study the flow, the sediment distribution, and the
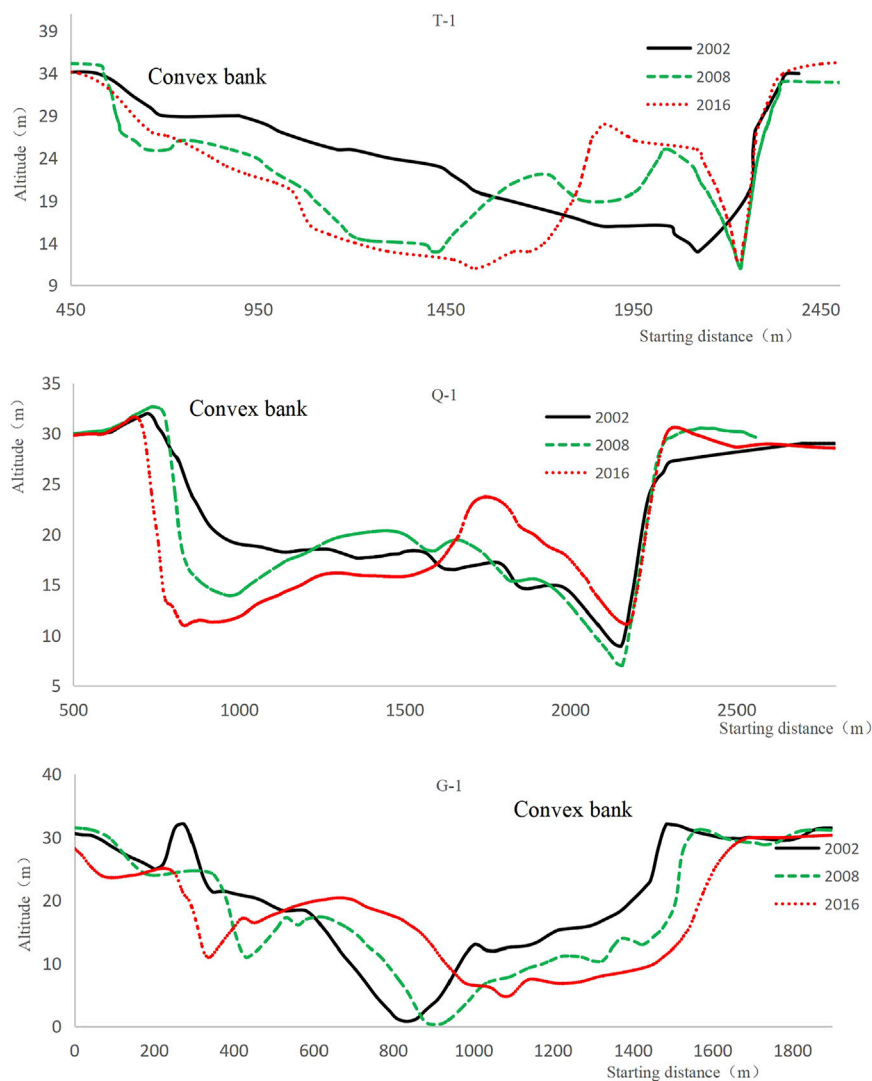
FIGURE 3
Change of the morphology of the studied river cross sections **(A)** T-1, **(B)** Q-1, and **(C)** G-1.
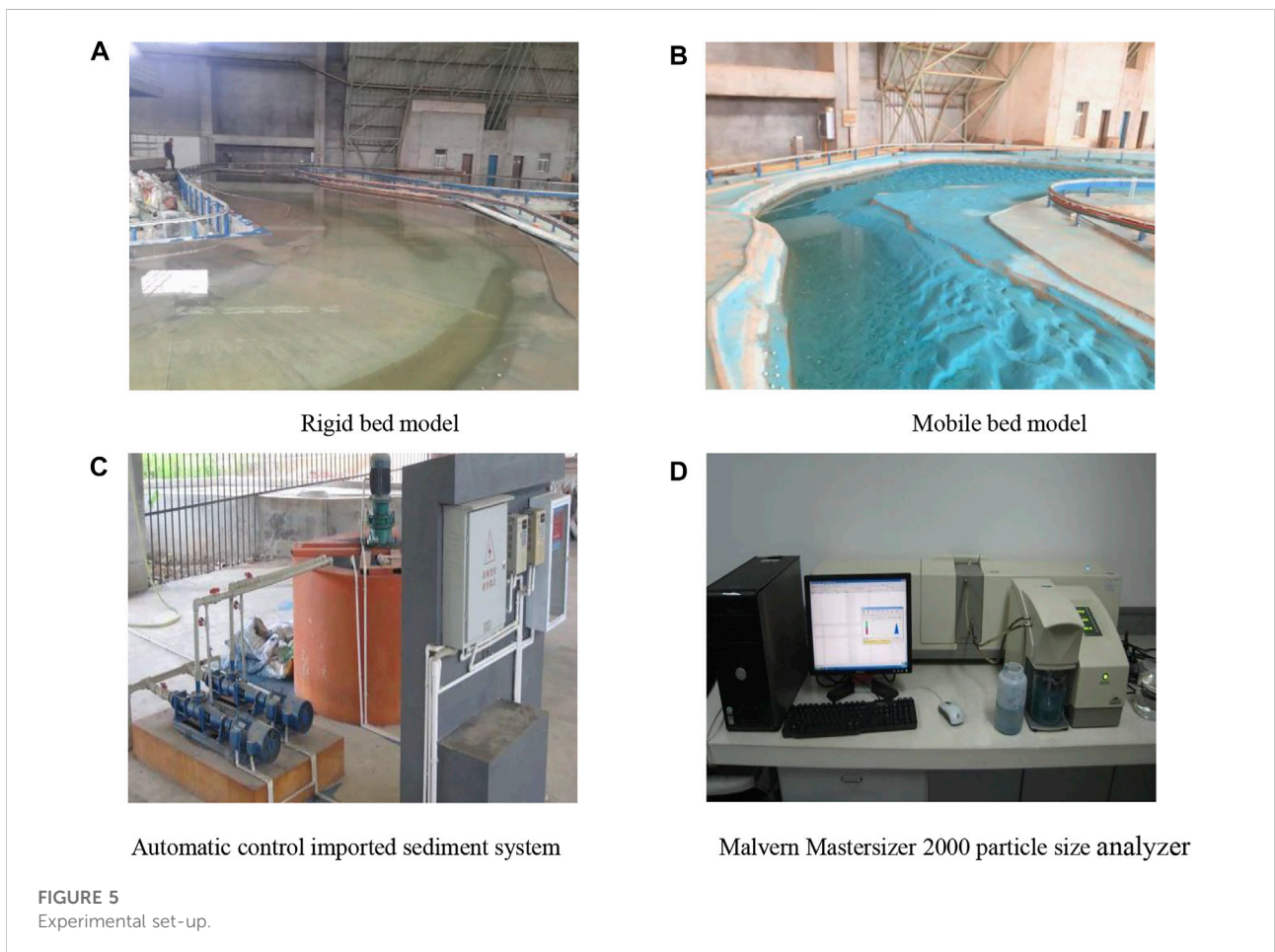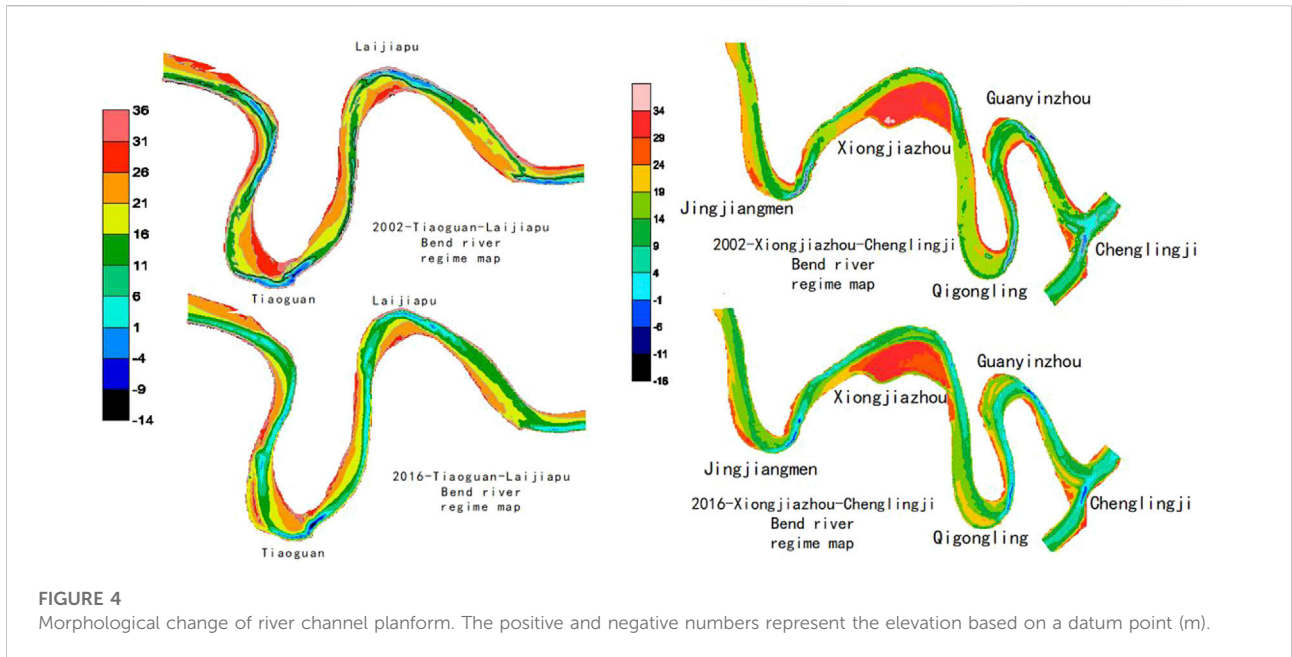
topographic change of the meandering channel under the condition of sediment reduction through the physical model experiment.

3 Physical model experiment

3.1 Experimental equipment

The experiments are conducted in the Ministry of Water Resources Key Laboratory of River and Lake Control and Flood Control in the Middle and Lower Reaches of the Yangtze River at the Yangtze River Scientific Research Institute, Wuhan, China. The scope of the model experiment is the Tiaoguan-Laijiapu

meandering reach of the Yangtze River. The full length of the prototype is about 40.8 km, and the length of the model is 102 m. The composition of the water and sediment supply system for the model experiment includes water circulation system, sediment circulation system, flow regulating equipment, desilting basin, side leaf adjustable tailgate, measuring equipment, and other auxiliary equipment. The composition of the water circulation system includes reservoirs, pumps, water pipelines, and backwater channels. The composition of the sediment circulation system includes reservoirs, pumps, a stir pool, a sediment transport pipeline, and an add-on sediment pump. The model adopts an electromagnetic flowmeter to measure and control the inlet flow. In order to ensure that the water flowing into the experimental section is as smooth as

FIGURE 4
Morphological change of river channel planform. The positive and negative numbers represent the elevation based on a datum point (m).
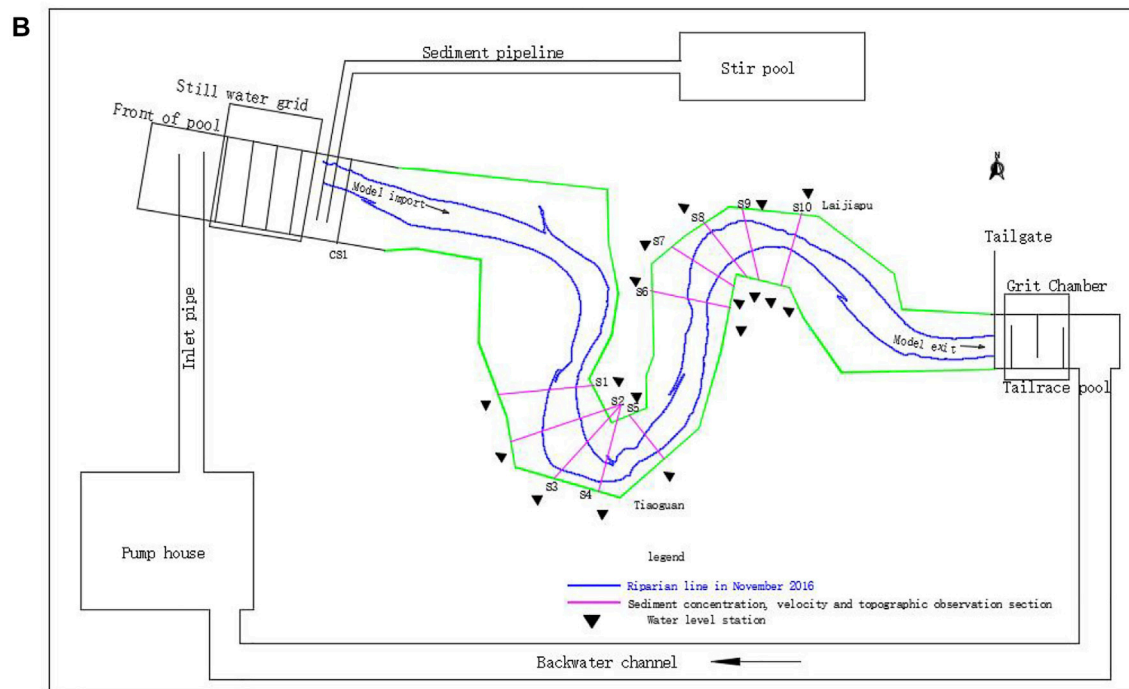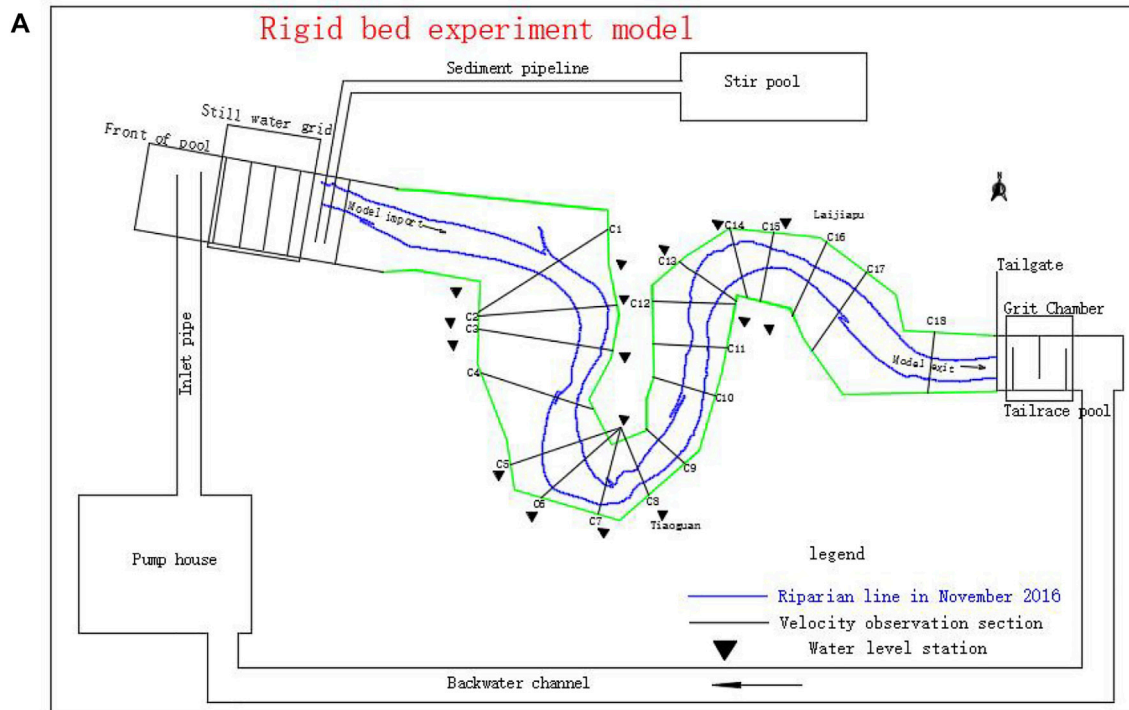

FIGURE 5
Experimental set-up.

FIGURE 6
Schematic diagrams illustrating the set-up of the experimental model.

possible, the model inlet section is equipped with a forebay with a flower wall and a steady flow grid. A transition section of about 3 m is set in front of the experiment section. The measuring equipment used in the experiment included the sediment sampler, the ADV three-dimensional flowmeter, the Malvern Mastersizer 2000 particle size analyzer, using laser diffraction technology to measure the particle size of sediment, the automatic water level meter, the electromagnetic flowmeter, and the electronic balance (Figure 5).

3.2 Model set-up and validation

The model experiment includes two schemes: 1) a rigid bed (Figure 6A) and 2) a mobile bed (Figure 6B). Using the rigid bed experiment, we will mainly study the flow variation characteristics of the meandering channel under different flow levels, whereas the mobile bed is suitable to investigate the sediment distribution characteristics and topographic change characteristics of the meandering channel under different sediment inflow conditions.

In order to fulfill the accuracy of the experiment, to improve the similarity between the research reach and the solid model, and to better follow the flow movement and riverbed evolution characteristics of natural rivers, the similarity of various factors must be fully considered in the experiment design, and each similar scale should be checked.

To ensure that the model and prototype flow are sufficiently described by the same physical equation, the model must satisfy the geometric similarity. Therefore, the model flow needs to fulfill the following two constraints:

1) The model flow must be turbulent, and the model Reynolds number R_{em} is greater than 1,000–2,000.
2) The surface tension does not interfere with the flow of the model, so the water depth of the model h_m is greater than 1.5 cm.

Under the current conditions, the water depth in the river channel of the studied reach is generally >2.5 m in the period of low flow, and the average velocity is about 1.2 m/s. The horizontal scale of 400 and the vertical scale of 100 are selected as the geometric scales of the model. A minimum Reynolds number of the model = 2,147 > 1,000–2,000 is calculated for the model, and the minimum water depth of the model is 2.5 cm > 1.5 cm, which satisfies the requirements. Based on this data, we calculated the flow movement scale to ensure that the flow inertia force, gravity, inertia force resistance, and flow continuity of the model are similar to those of the prototype.

The similarity of flow movement in the model must meet the inertia force gravity similarity (Eq. 1), the inertia force resistance similarity (Eq. 2), and the continuity similarity of flow (Eq. 3).

$$\alpha_V = \alpha_H^{\frac{1}{2}} \tag{1}$$

$$\alpha_n = \alpha_H^{\frac{2}{3}} \Big/ \alpha_L^{\frac{1}{2}}, \tag{2}$$

$$\alpha_Q = \alpha_H \alpha_H \alpha_V. \tag{3}$$

According to the purpose and requirements of the experiment, bed load and suspended load shall be modeled simultaneously. For the suspended load, the bed material load part in the suspended load mainly affects the scouring and silting change of the riverbed. The amount of bed load in the studied reach is far less than that of bed material load. Therefore, the similarity of bed material load movement in suspended load is mainly considered in the model design. Based on these findings, we will determine the basic conditions for similar sediment movement. Due to the purpose of the experiment, the model mainly considers the scouring problem of the studied reach. Therefore, the model set-up is mainly based on the premise of satisfying the similar conditions of sediment incipient movement. According to the measured data of the prototype river reach, the boundary particle size between bed material load and wash load in the suspended load of the river reach is 0.05 mm, and the average median particle size of bed material load in the suspended load is 0.195 mm. The median particle size of the prototype bed material is 0.15–0.23 mm, and the average particle size is about 0.194 mm.

The incipient velocity of prototype sediment is calculated by Eq. 4 (Sha Yuqing formula) and the incipient velocity of the model sediment by Eq. 5. The fitting formula of the flume experiment results from the study of Zhou (2015).

$$u = \left[0.43 d^{\frac{3}{4}} + 1.1 \frac{(0.7 - e)^4}{d} \right]^{\frac{1}{2}} h^{\frac{1}{5}}, \tag{4}$$

$$U = 0.9216 \left(\frac{H}{d_{50}} \right)^{0.141} \left(17.6 \frac{\gamma_s - \gamma}{\gamma} d_{50} + 0.000000016 \frac{10 + H}{d_{50}^{0.885}} \right)^{1/2} - 2.105. \tag{5}$$

The calculated incipient velocity of prototype bed sediment is 0.587–0.841 m/s, and the calculated incipient velocity of model bed sediment is 6.45–8.93 cm/s for water depths of 5–30 m and a model bed sediment median particle size of $d_{50} = 0.254$ mm. The incipient velocity scale of bed sediment is 9.11–9.42, and it is only slightly lower than the velocity scale of 10, indicating that the selected model sediment basically satisfies the incipient similar conditions. According to the incipient similarity criterion, a value of 0.9 is determined for the particle size scale of the model, and the median particle size of the model bed sediment is calculated as 0.22 mm. The design grading curve of bed sediment in the model is shown in Figure 7. The final values of sediment concentration and sediment transport rate scale are determined through the model validation experiment results. The model sediment used in this experiment is synthetic plastic sediment, and the bulk density is designed as 1.38 t/m³. The dry
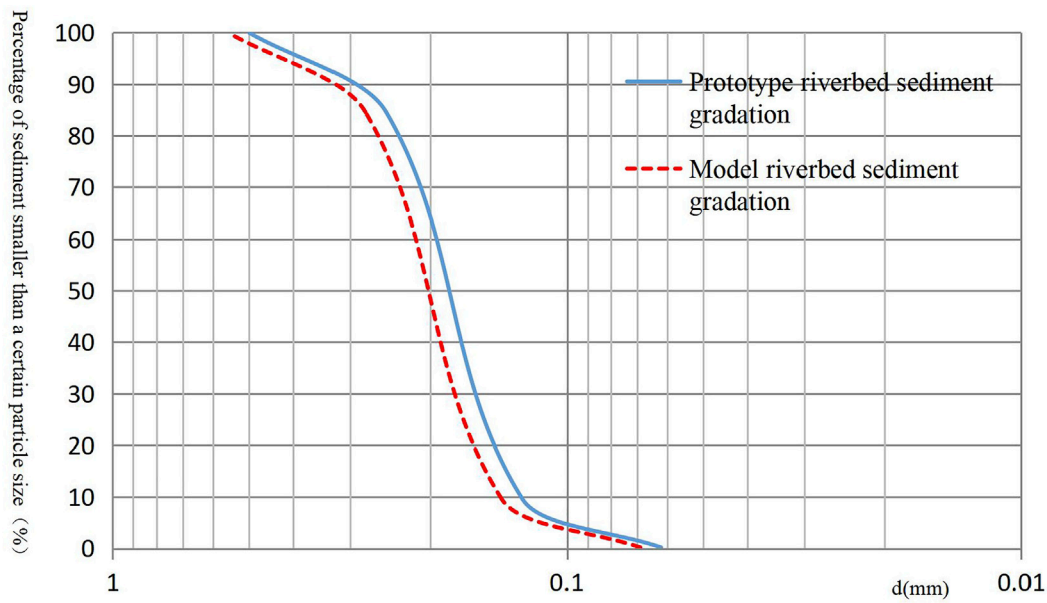
FIGURE 7
Design grading curve of bed sediment in the model.

TABLE 3 Model scale selection.

Similitude consideration	Scale name	Symbol	Ratio
Geometric similarity	Horizontal	α_L	400
	Vertical	α_H	100
	Velocity	α_V	10
	Roughness	α_n	1.08
Similarity of flow movement	Rate of flow	α_Q	400,000
	Time of flow	α_{t_1}	40
	Subsiding velocity	α_ω	2.5
	Dry capacity	α_{γ_0}	2.02
Similarity of suspending sediment movement	Particle size	α_d	0.9
	Sediment concentration	α_s	0.442
	Riverbed deformation time	α_{t_2}	183
	Subsiding velocity	α_ω	2.5
	Dry capacity	α_{γ_0}	2.02
	Particle size	α_d	0.9
Similarity of bed load movement	Starting velocity	α_{V_0}	10
	Bed load transport rate per unit width	α_{q_b}	442
	Riverbed deformation time	α_{t_3}	183

bulk density changes slightly with the change in model sediment particle size. The value is 0.65 t/m³.

We selected water levels of the Shashi hydrological station under a flow of 40,100 m³/s on 20 July 1998, 28,600 m³/s on 24 July 2008, and 11,400 m³/s on 29 May 2011 for verification of the experiment. The water level may be affected by the bank roughness under different flow levels. A minor difference between the natural measured water level and the model water level is observed, and the difference increases at the tail of the model. However, the difference between the natural river

TABLE 4 Rigid bed experiment flow conditions.

Case	Prototype flow (m³/s)	Model flow (dm³/s)	Control water level (cm)	Control section area (cm²)	Control section velocity (cm/s)
A	5,000	12.5	23.7	1,514	8.26
B	11,400	28.5	28.79	2,067	13.79
C	20,000	50	32.86	2,602	19.22
D	28,000	70	35.58	3,120	22.44
E	40,000	100	38.7	4,119	24.28

TABLE 5 Flow and sediment conditions of mobile bed experiment.

Typical year	Prototype generalized flow (m³/s)	Sediment transport rate of prototype (kg/s)	Duration of each flow level (min)	Model generalized flow (dm³/s)	Sediment transport rate of model (g/s) 100%	50%	0%	Model tailgate control water level (1,985 mm)	Trial monitoring
1998	4,355	239.745	120	11	0.799	0.4	0	241.28	
	7,008	726.134	341	18	2.42	1.21	0	255.98	
	12,267	2,675.452	512	31	8.918	4.459	0	289.58	
	33,952	**28,660.764**	**864**	**85**	**95.536**	**47.768**	**0**	**357.08**	Sediment concentration
	14,572	**3,995.688**	**576**	**36**	**13.319**	**6.66**	**0**	**292.48**	Topography
	7,593	875.236	160	19	2.917	1.459	0	250.28	
	5,844	475.625	120	15	1.585	0.793	0	238.28	
	5,233	459.682	120	13	1.532	0.766	0	233.18	
	7,555	1,081.333	363	19	3.604	1.802	0	252.08	
	11,155	2,680.252	320	28	8.934	4.467	0	269.88	
	13,115	3,907.774	437	33	13.026	6.513	0	285.98	
	19,270	9,576.426	395	48	31.921	15.961	0	304.48	
2008	**23,614**	**15,376.63**	**459**	**59**	**51.255**	**25.628**	**0**	**320.88**	Sediment concentration
	15,559	**5,818.381**	**288**	**39**	**19.395**	**9.698**	**0**	**291.48**	Topography
	8,282	1,339.381	160	21	4.465	2.233	0	252.98	
	14,063	4,597.618	256	35	15.325	7.663	0	289.98	
	7,037	916.441	213	18	3.055	1.528	0	243.88	
	8,197	1,307.579	619	20	4.359	2.18	0	247.58	
	12,266	3,343.68	373	31	11.146	5.573	0	274.88	
	17,673	**7,828.608**	**672**	**44**	**26.095**	**13.048**	**0**	**298.58**	Sediment concentration
2011	**12,153**	**3,272.365**	**384**	**30**	**10.908**	**5.454**	**0**	**271.28**	Topography
	8,934	1,597.962	352	22	5.327	2.664	0	255.58	
	14,093	4,620.496	149	35	15.402	7.701	0	272.78	
	7,439	**1,043.052**	**469**	**19**	**3.477**	**1.739**	**0**	**244.58**	Topography

The black numbers indicate that we have carried out the measurement under this working condition.
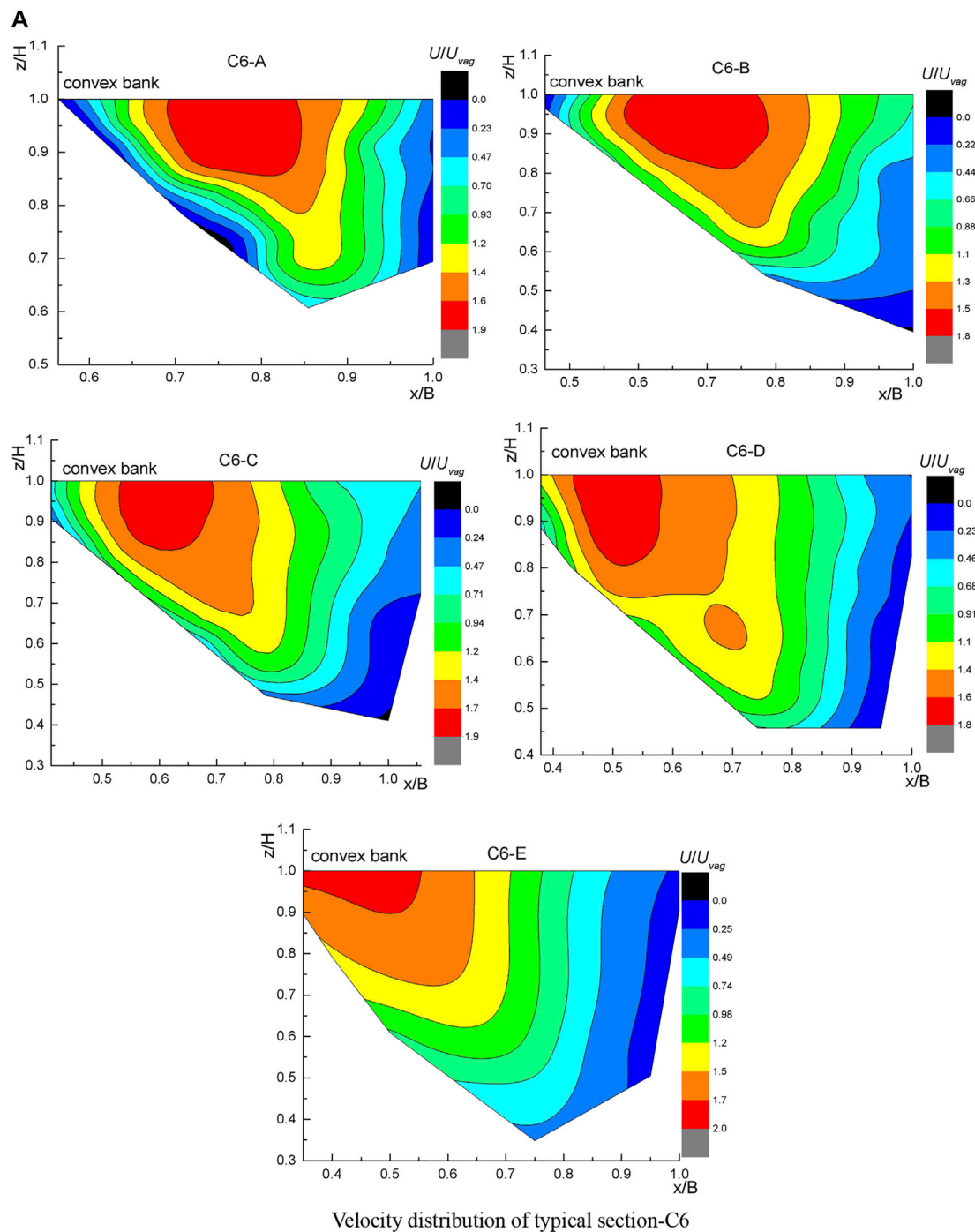
FIGURE 8
Velocity distribution of typical section.

water level and the verified water level is less than 1 mm, which is within a reasonable error range. The initial riverbed landform of the model verification experiment is made of 1: 10,000 underwater landforms measured in November 2011.

The model validation experiment releases the flow and sediment process of the Shashi hydrological station from November 2011 to October 2013 to reproduce the measured riverbed landform in October 2013. The results of the verification

FIGURE 9
Variation of the dynamic axis of flow under different flow levels.
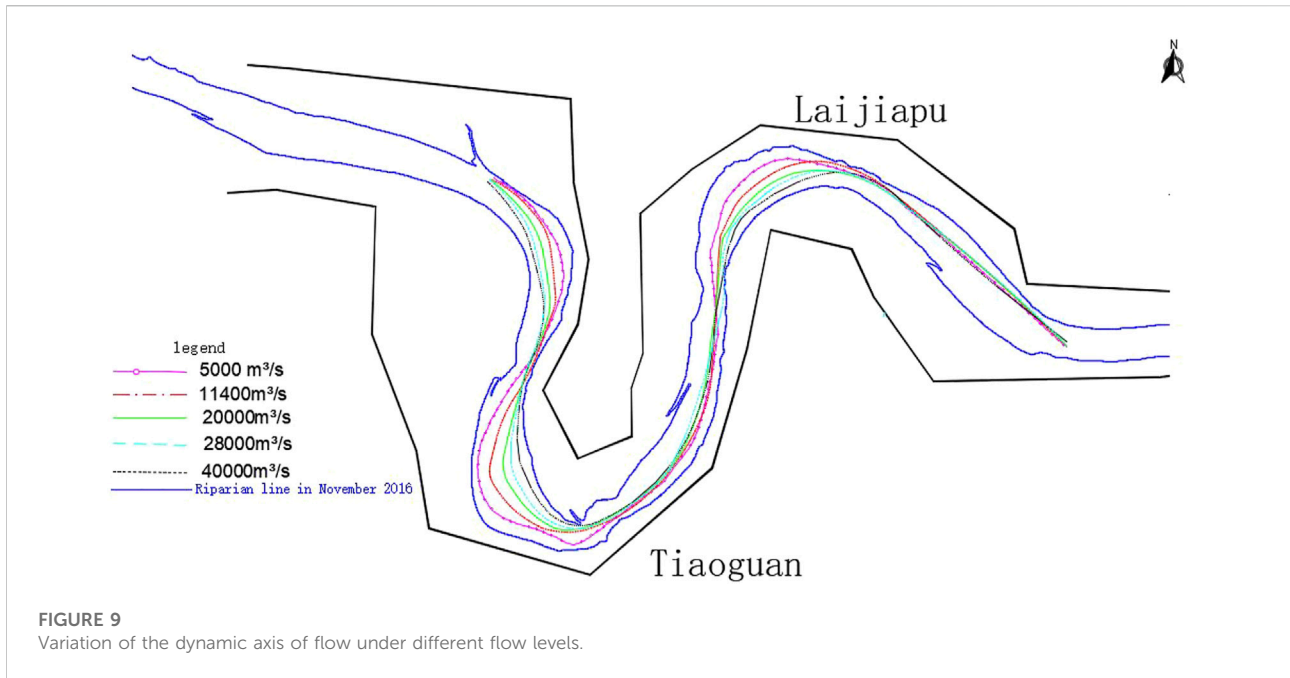
experiment show that the model reproduces the principles of erosion, deposition, and sediment movement of the prototype shoal and channel sufficiently. Moreover, the thalweg position and cross-section shape of the model are generally consistent with those of the prototype. The results of the validation experiment demonstrate that the design of the model, the selection of sediment, and the selection of various scales are reasonable. Through the validation experiment, all parameters, including sediment concentration, sediment transport rate, and scouring and silting time of the model, are accurately determined (Table 3).

3.3 Experimental program

The experiment has been subdivided into two parts: the first part is the rigid bed experiment. Five groups of working conditions have been selected for the experiment, including large, medium, and low flow levels (Table 4). The C1–C17 sections, marked in Figure 6A, have been selected as the velocity measurement section. The 10–15 vertical lines have been chosen for each cross section for measurement, and the measuring points of each vertical line were distributed according to the water depth, with one measuring point every 2 cm. The second part is the mobile bed experiment. For the mobile bed experiment, we have selected the 2016 1: 10,000 landform to initially constitute the mode. In the experiment, we used the measured flow and sediment processes of the Shashi hydrological station in 1998 (high flow year), 2008 (medium flow year), and 2011 (low flow year)

(Table 5). In the experiment, we utilized sediment discharge as the control factor, and we selected three working conditions of 100, 50, and 0% sediment discharge, respectively. The S1–S10 sections, illustrated in Figure 6B, have been selected as the topographic and sediment concentration monitoring sections. The selection of sediment concentration measurement points has been the same as the earlier described velocity measurement. The sediment concentration has been calculated by the drying and weighing method, and the landform has been monitored by a topographic instrument (invented by the Yangtze River Scientific Research Institute and Wuhan University).
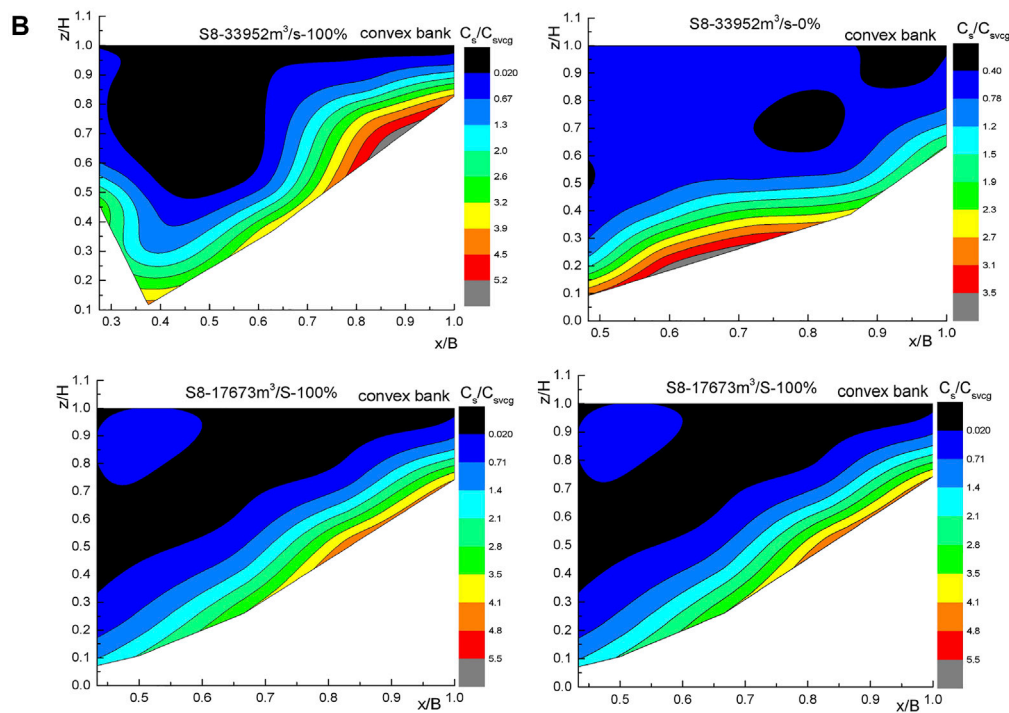
4 Results

4.1 Flow characteristics

The C6 and C14 sections (Figure 6A) have been selected for a detailed velocity analysis as they represent typical sections. The chosen section is located near the upper position of the bend top of the two bends, which can reflect the distribution characteristics of the cross-sectional velocity. The two observation sections show very similar change features (Figure 8): With the increase of the flow level, the main flow area gradually shifts toward the convex bank. The main difference is the lower degree of curvature of the C14 section. The main flow area shifts toward the convex bank with increasing flow level, but the range of movement is lower than that of the C6 section. This observation implies different constraints on the flow movement related to the degree of
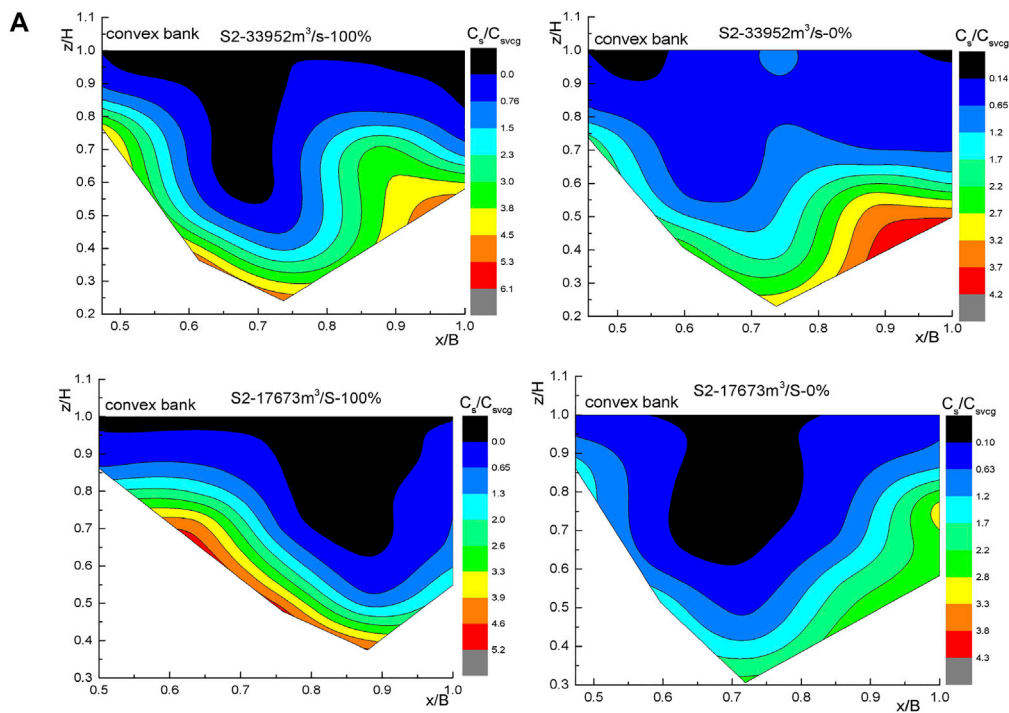
FIGURE 10
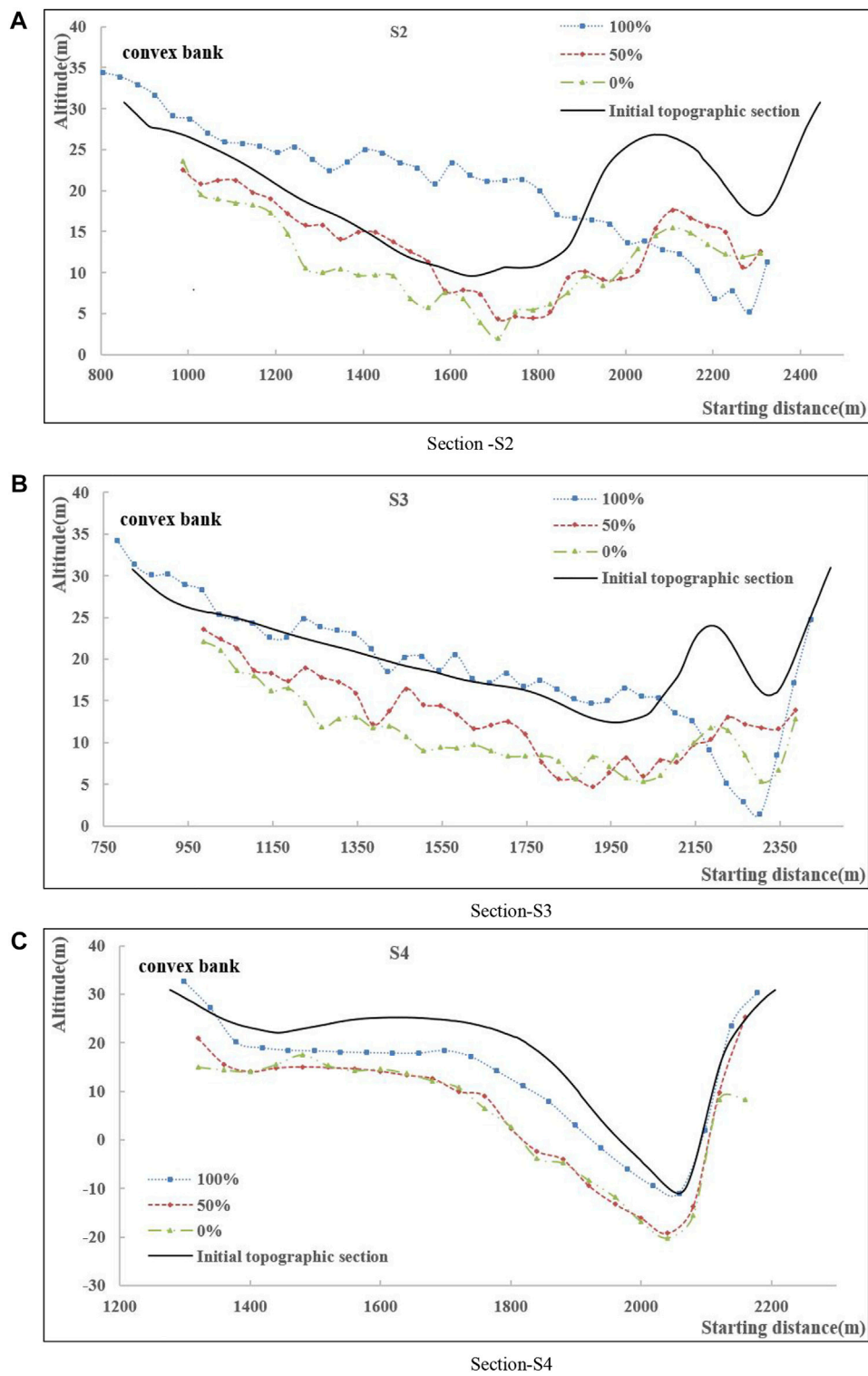Section distribution of sediment concentration.

FIGURE 11
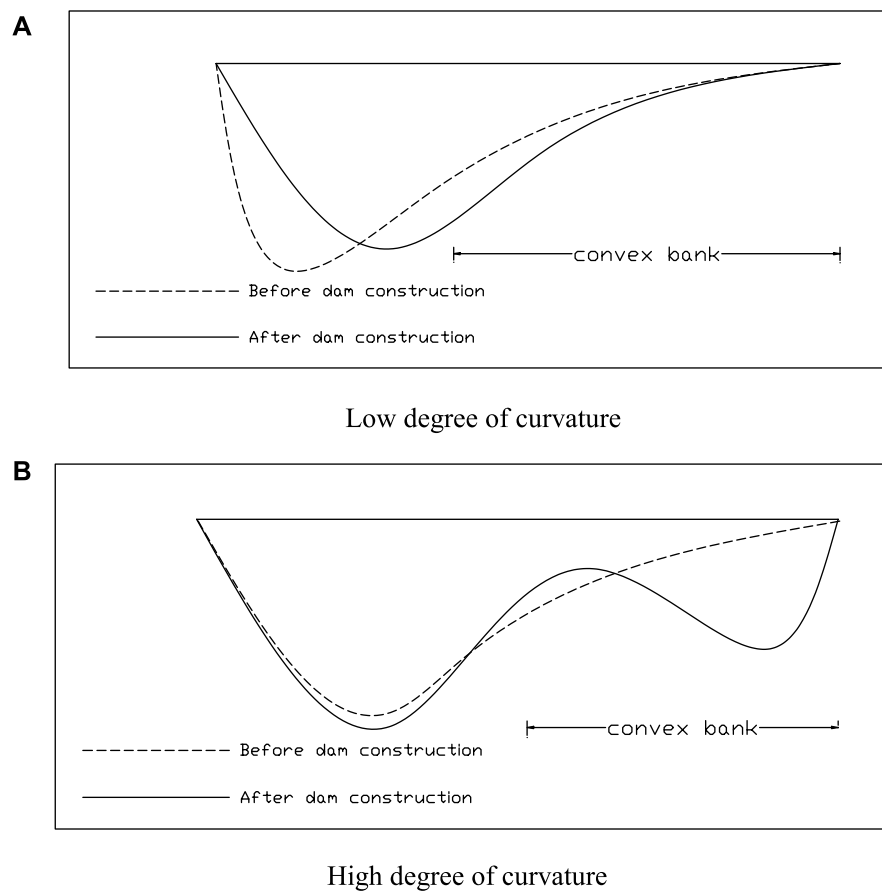Topographic change of selected sections.

FIGURE 12
Topographic section changes of river channel with different degrees of curvature.

curvature of the bend. For a low degree of curvature of the bend, the restriction degree of the river channel to the flow movement is inferior at the same flow level condition. Otherwise, the results are the opposite. For the same bend, the constraint of river boundary conditions on flow decreases gradually with increasing flow level.

In previous studies, the swing law of the dynamic axis of flow in the meandering channel has been attributed to the incoming flow and the type of bend. It has been termed the law of "low water near the bank, high water swinging to the middle of the river" (Zhang et al., 2021). According to our experimental results (Figure 9), the dynamic axis of flow swings from the concave bank to the convex bank in the two bends with the increase of the flow level, which is the same as the distribution law of the section velocity. The radii of curvity of the Tiaoguan bend and the Laijiapu bend are 1,062 m, and 1,524 m, respectively, as obtained by the trial circle method. For a bend with a different radius of curvity, the motion trajectories of the dynamic axis of flow are different under the same flow level. For the bend with a small radius of curvity, the position of the dynamic axis of flow is close

to the convex bank, whereas for the bend with a large radius of curvity, it is close to the concave bank.

The variation of the dynamic axis of flow is generally characterized by the inlet section of the bend being close to the convex bank. Subsequently, the dynamic axis of flow gradually shifts to the concave bank to reach the nearest point (vertex scouring position) from the concave bank. Finally, it gradually returns to the convex bank at the outlet of the bend. With the increase of flow level, the radius of the dynamic axis of flow decreases gradually, and the vertex scouring position declines gradually, showing a trend of swinging toward the convex bank. The swing range is large at the top of the bend and small at the inlet and outlet. Our experimental results demonstrate that the swing characteristics of the dynamic axis of flow are consistent with the law of "low water near the bank, high water swinging to the middle of the river" proposed in previous studies. Compared with the bend with a larger radius of curvity, the vertex scouring position of the dynamic axis of flow moves downstream of the bend for the bend with a smaller radius of curvity, and the radius of curvity of the dynamic axis of flow is

comparably small. For the same flow conditions, the swing range of the dynamic axis of flow is large under the different flow level conditions for the bend with a large degree of curvature, and the position with the largest swing range is on the upper part of the bend top. On the contrary, for the bend with a small degree of curvature, the swing range of the dynamic axis of flow is comparably small, and the position with the largest swing range is on the bend top.

4.2 Variation of distribution of the sediment concentration

The results of the rigid bed model experiment show that the dynamic axis of flow is located at the concave bank for a low flow level. In contrast, the dynamic axis of flow swings to the convex bank of the bend at a high flow level. We have selected the S2 and S8 sections, indicated in Figure 6B, to analyze the distribution characteristics of sediment concentration sections at flow levels of 33,952 m^3/s and 17,673 m^3/s, respectively (Table 5), and sediment inflow between 100 and 0% (Figure 10). The experiment results show an inhomogeneous distribution of the sediment concentration of the meandering river section. The sediment concentration increases gradually from the water surface to the riverbed. Moreover, the sediment concentration is much higher near the riverbed than at the water surface, which is in line with the characteristics of "small at the top and large at the bottom" as recognized in previous studies (Liu, 2007).

For 00% sediment inflow, the sediment concentration distribution of the two sections shows a higher sediment concentration on the convex bank than on the concave bank. With the reduction of incoming sediment, the main sediment transport belt shifts from the convex bank toward the concave bank. For 0% sediment inflow, the sediment concentration on the convex bank is lower than that on the concave bank. The observed phenomena are generally similar under the conditions of two flow levels. The sediment in the flow mainly derives from the upstream and riverbed. In the situation of sufficient incoming sediment, due to the influence of transverse circulating flow, the sediment concentration at the convex position is higher than that at the concave bank. The convex bank is silted, whereas the concave bank is scoured. For very low sediment inflow in the upstream reach, the sediment is mainly derived from the riverbed. The experimental results show that the sediment concentration on the concave bank is greater than that on the convex bank. In order to satisfy the sediment carrying capacity of the flow, the convex bank may be scoured.

4.3 Topographic change

The S2, S3, S4, S7, S8, and S9 sections, shown in Figure 6B, have been selected for an analysis of the landform change

characteristics (see Figure 11). The selected sections are located at the top of the bend as well as above and below the top of the bend. The main factors affecting the landform change of the cross section of the bend include the degree of curvature of the meandering channel and the sediment inflow upstream. In the situation of sufficient incoming sediment, the evolution of the bend basically conforms to the evolution law of concave bank scouring and convex bank silting. At first, we discuss the bend with a large degree of curvature (Figures 11A–C). The landform evolution of the river channel at the bend top and the upper part of the bend top is radical. With the decrease of incoming sediment, the convex bank of the bend is scoured, the concave bank is silted, and the main channel swings toward the convex bank. In addition, the cross section of the upper channel at the bend top gradually changes to W shape. At the lower part of the bend top, with the decrease of incoming sediment, the river channel is generally scoured, and the V shape of the cross section of the river channel remains unchanged.

For bend with a small degree of curvature (Figures 11D–F) at the upper part of the bend top, the convex bank is silted, and the channel becomes narrower with the decrease in incoming sediment. The evolution of the bend top position is drastic. The convex bank of the channel at the bend top position and the lower part of the bend top position are scoured, and the main channel is deeply brushed and widened with the decrease of incoming sediment. The river cross section of the entire bend is V-shaped.

5 Discussion

5.1 Coupling mechanism

According to our prototype data observation and the results of our model experiment analysis, the flow and sediment conditions in the lower reaches of a river will significantly change, and the landform characteristics of the river will be adjusted to the new situation after the construction of a river barrage in the upper reaches of the river. The phenomenon of sediment inflow reduction in the river downstream of dams after the construction of a barrage is common in several other rivers (Li et al., 2015; Chen et al., 2018). Taking the meandering channel as an example, the change of the landform characteristics of the river channel is mainly related to the shape and boundary conditions of the meandering channel itself as well as the flow and sediment inflow conditions in the upper reaches of the river channel.

We have studied the meandering river in the lower reaches of the Three Gorges Reservoir of the Yangtze River in China as a prototype observation reach. According to prototype observation, the evolution characteristics of bend bypassing and shoal cutting were initiated in the downstream reach after

the operation of the Three Gorges reservoir. Theoretical analysis and model experimental research indicate that the flow process changes significantly after the operation of the Three Gorges reservoir. Flow levels <5,000 m³/s and >25,000 m³/s have decreased, whereas flow levels >5,000 m³/s and <25,000 m³/s have increased. The rigid bed model experiment results show that with the increase in flow level, the dynamic axis of flow swings to the convex bank. Therefore, the duration of the dynamic axis of flow being located on the convex bank has increased after the operation of the Three Gorges reservoir, providing dynamic conditions for the scouring of the convex bank of the meandering river. The results of the mobile bed model experiment indicate that with the decrease of incoming sediment, the sediment concentration on the convex bank at the top of the bend is lower than that on the concave bank, and the convex bank is scoured. The data document that as the sediment inflow from the upstream decreases, the sediment concentration on the convex bank is lower than the sediment carrying capacity of the flow, and the convex bank is subject to cumulative scouring. Hence, a gradual decrease of the incoming sediment causes scouring of the convex bank of the meandering river, and the central bar may appear near the concave bank.

To summarize, the reduction of the incoming sediment is the main cause for the change of the landform characteristics of the meandering river, as it disturbs and ultimately destroys the natural equilibrium of river beach and river channel sediment transport in the meandering river. In previous studies, the discussion of the evolution of the meandering channel was mostly based on the condition of sediment transport balance. In our study, we consider the conditions of sediment transport imbalance, which can provide a reference for the discussion of riverbed deformation during sediment reduction in comparable rivers.

5.2 Meandering channel deformation model

Previous studies have mostly used generalized bends with the same shape and size (Shiono et al., 2008; Wang et al., 2022). In our study, we have considered that natural rivers are composed of different types of bends, and we have analyzed the changes of the bend section under conditions of the reduced amount of incoming sediments, Therefore, our study may provide a solid reference for the study of comparable rivers. With a different degree of curvature of the bend, the swing range of the dynamic axis of flow is different from the flow levels; hence, the landform characteristics of the river channel are adjusted to different patterns. Two main patterns are distinguished, that is, the cross-section change of bends with a high degree of curvature and bends with a low degree of curvature (Figure 12). For bends with a low degree of curvature, the swing range of the dynamic axis of flow changes slightly with the flow levels. The exchange frequency between sediment carried by flow and bed sediment is low, and the deformation range of riverbed

landforms is generally minor. The dynamic axis of flow swings at the top of the bend; hence, the river channel landform changes markedly at the top of the bend. Due to the low swing range of the dynamic axis of flow, the change range of the river topography is very moderate, and the cross section of the river topography is V-shaped under the condition of reduced sediment inflow (Figure 12A). For bends with a high degree of curvature, from the entrance of the bend to the top of the bend, the swing range of the dynamic axis of flow is large, and the exchange frequency between sediment carried by flow and riverbed sediment is particularly high. Therefore, the evolution range of landform at the upper part of the bend top is large, and the cross section of riverbed landform changes from V shape to W shape under the condition of reduced sediment inflow (Figure 12B).

6 Conclusion

Based on the theoretical analysis of measured data and a physical experimental model, we have deciphered the coupling mechanism of the river landform change characteristics of the meandering river and the variation of flow and sediment conditions induced by the reduction of sediment inflow. We have derived the following findings:

The construction of river barrages changes the flow and sediment conditions in the downstream reach. After the construction of the Three Gorges Reservoir in China, the average annual runoff of the lower reaches of the reservoir has slightly decreased, but the incoming flow process has changed significantly. The main consequences have been the reduction of floods and extremely low flow levels, whereas the occurrence frequency of medium and low flow levels has significantly increased. In addition, the sediment transport and interannual average daily sediment concentration have decreased significantly.

The swing range of the dynamic axis of flow is closely related to the flow and the plane shape of the bend. Large swing ranges of the dynamic axis of flow occur near the bend inlet to the bend top and gradually close together at the lower part of the bend top. Therefore, the channel evolution from the inlet to the top of the bend is significant.

After the construction of the river barrage, the change of flow conditions provides dynamic conditions for the phenomenon of bend bypassing and shoal cutting in the meandering channel downstream of the river barrage. The sediment concentration of the flow decreases significantly, which is caused by sediment intercepted by river barrages and the change in the environment. The sediment transport capacity of flow is much higher than that of the sediment inflow. These are the main factors for the bend bypassing and shoal cutting in the meandering channel of the natural alluvial river.

The degree of curvature of the meandering channel is large under the influence of sediment reduction. The dynamic axis of

flow swings to the convex bank with the increase of the flow level, and the swing range is high. Therefore, the convex bank is scoured, and the concave bank of the river channel is silted to form a central bar. Therefore, the cross-section shape of the river channel transforms from V shape to W shape. For a low degree of curvature of the meandering channel, the dynamic axis of flow swings to the convex bank with the increase of flow level, and the swing range is low. The convex bank is gradually scoured, and the concave bank is gradually silted. The topographic cross section of the river channel remains V-shaped.

Data availability statement

The original contributions presented in the study are included in the article/Supplementary Material; further inquiries can be directed to the corresponding author.

Author contributions

All authors listed have made a substantial, direct, and intellectual contribution to the work and approved it for publication.

Funding

Conflict of interest

The authors declare that the research was conducted in the absence of any commercial or financial relationships that could be construed as a potential conflict of interest.

Publisher's note

All claims expressed in this article are solely those of the authors and do not necessarily represent those of their affiliated organizations, or those of the publisher, the editors, and the reviewers. Any product that may be evaluated in this article, or claim that may be made by its manufacturer, is not guaranteed or endorsed by the publisher.

References

Amirhossein, A., Alireza, K., Hossein, H., and Javan, M. (2020). Effect of rigid vegetation on velocity distribution and bed topography in a meandering river with a sloping bank[J]. *Arabian J. Sci. Eng.* 45, 8633–8653. doi:10.1007/s13369-020-04818-7

Arnez, F. K. R., Nelson, J. M., Shimizu, Y., and Kyuka, T. (2021). Past, present and future of a meandering river in the Bolivian Amazon basin[J]. *Earth Surf. Process. Landforms* 46 (4), 715–727. doi:10.1002/esp.5058

Braudrick, C. A., Dietrich, W. E., Leverich, G. T., and Sklar, L. S. (2009). Experimental evidence for the conditions necessary to sustain meandering in coarse-bedded rivers. *Proc. Natl. Acad. Sci. U. S. A.* 106 (40), 16936–16941. doi:10.1073/pnas.0909417106

Chen, L., Song, T., Lu, S. Y., and Bing, J. P. (2018). Analysis of Single scouring characteristics for typical bend reaches in lower Hanjiang River. *Eng. J. Wuhan Univ.* 51 (04), 283–288. doi:10.14188/j.1671-8844.2018-04-001

Constantine, J. A., Dunne, T., Ahmed, J., Legleiter, C., and Lazarus, E. D. (2014). Sediment supply as a driver of river meandering and floodplain evolution in the Amazon Basin. *Nat. Geosci.* 7 (12), 899–903. doi:10.1038/ngeo2282

Darby, S. E., Alabyan, A. M., and Wiel, M. J. V. D. (2002). Numerical simulation of bank erosion and channel migration in meandering rivers. *Water Resour. Res.* 38 (9), 2-1–2-21. doi:10.1029/2001wr000602

Dietrich, W. E., and Smith, J. D. (1984). Bed load transport in a river meander. *Water Resour. Res.* 20 (10), 1355–1380. doi:10.1029/wr020i010p01355

Donatella, T., and Mafalda, P. (2011). Experimental analysis of cross-sectional flow motion in a large amplitude meandering bend[J]. *Earth Surf. Process. Landforms* 36 (2), 244–256. doi:10.1002/esp.2095

Fan, Y. Y., Zhang, W., Han, J. Q., and Yu, M. Q. (2017). Regulation of the evolution law of the bending river pattern in the lower reaches of the Three Gorges Reservoir and its driving mechanism. *J. Geogr.* 72 (03), 420–431. doi:10.11821/dlxb201703005

Fisk, H. N. (1945). Geological investigation of the alluvial valley of the lower Mississippi river[J]. *J. Geol.* 37 (1), 166–167.

Frascati, A., and Lanzoni, S. (2009). Morphodynamic regime and long-term evolution of meandering rivers. *J. Geophys. Res.* 114 (F2), F02002. doi:10.1029/2008jf001101

Furbish, D. J. (1991). Spatial autoregressive structure in meander evolution. *Geol. Soc. Am. Bull.* 103 (12), 1576–1589. doi:10.1130/0016-7606(1991)103<1576:sasime>2.3.co;2

Güneralp, İ., and Rhoads, B. L. (2011). Influence of floodplain erosional heterogeneity on planform complexity of meandering rivers[J]. *Geophys. Res. Lett.* 38 (14), 130–137. doi:10.1029/2011GL048134

Harmar, O. P., and Clifford, N. (2010). Planform dynamics of the lower Mississippi river[J]. *Earth Surf. Process. Landforms* 31 (7), 825–843. doi:10.1002/esp.1294

Hooke, J. M., and Yorke, L. (2011). Channel bar dynamics on multi-decadal timescales in an active meandering river. *Earth Surf. Process. Landf.* 36 (14), 1910–1928. doi:10.1002/esp.2214

Kassem, A. A., and Chaudhry, M. H. (2002). Numerical modeling of bed evolution in channel bends. *J. Hydraul. Eng.* 128 (5), 507–514. doi:10.1061/(asce)0733-9429(2002)128:5(507)

Keshavarzi, A., Hamidifar, H., and Ball, J. (2016). Bed morphology in vegetated estuarine river with mild-curved meander bend. *Hydrological Sci. J.* 61 (11), 2033–2049. doi:10.1080/02626667.2015.1081201

Li, N. B., Zeng, Y., and Wu, Z. M. (2013). Preliminary study on the causes of the bending of Qigongling main stream in Jingjiang section of the Yangtze River. *People's Yangtze River* 44 (01), 22–25. doi:10.16232/j.cnki.1001-4179.2013.01.018

Li, X. J., Xia, J. Q., Li, J., and Zhang, X. L. (2015). Variation in Bankfull Channel Geometry in the LYR Undergoing Continuous Aggradation and Degradation. *J. Sichuan Univ. Sci. Ed.* 47 (01), 97–104. doi:10.15961/j.jsuese.2015.01.014

Lindroth, E. M., Rhoads, B. L., Castillo, C. R., Czuba, J. A., Guneralp, I., and Edmonds, D. (2020). Spatial variability in bankfull stage and bank elevations of lowland meandering rivers: Relation to rating curves and channel planform characteristics. *Water Resour. Res.* 56 (8), e2020WR027477.1–e2020WR027477.24. doi:10.1029/2020WR027477

Liu, Q. Q. (2007). "Analysis of the vertical profile of concentration in sediment-laden flows. *J. Eng. Mech.* 133 (6). doi:10.1061/(ASCE)0733-9399(2007)133:6(601)

Luchi, R., Hooke, J. M., Zolezzi, G., and Bertoldi, W. (2010). Width variations and mid-channel bar inception in meanders: River Bollin (UK). *Geomorphology* 119 (1), 1–8. doi:10.1016/j.geomorph.2010.01.010

Qin, L. C., Yu, M. H., Tan, G. M., Xu, D., and Xiang, H. (2009). Study on the relationship between the change of flow dynamic axis and the abandonment of cut-off beach. *Hydrodynamics Res. Prog. Part A* 24 (01), 29–35.

Ruan, C. T. (2016). Evolution of beach and trough in sandy meandering reach under the condition of clear water discharge. *Waterw. Port.* 37 (04), 399–404. doi:10.3969/j.issn.1005-8443.2016.04.017

Sergio, L. D., and Stefano, L. (2019). Meandering evolution and width variations: A physics-statistics-based modeling approach[J]. *Water Resour. Res.* 55 (1), 76–94. doi:10.1029/2018WR023639

Shiono, K., Spooner, J., Chan, T., Rameshwaran, P., and Chandler, J. (2008). Flow characteristics in meandering channels with non-mobile. *J. hydraulic Res.* 46 (1), 113–132. doi:10.1080/00221686.2008.9521848

Sixuan, L., Yitian, L., Jing, Y., Zhang, W., Chai, Y., and Ren, J. (2018). The impacts of the Three Gorges Dam upon dynamic adjustment mode alterations in the Jingjiang reach of the Yangtze River, China. *Geomorphology* 318, 230–239. doi:10.1016/j.geomorph.2018.06.020

Wang, Q., Shan, Y. Q., Liu, C., and Liu, X. N. (2022). "Experimental study on characteristics of bed evolution and overbank floods in meandering channel under different water and sediment discharges," in *Advanced engineering sciences*, 1–11. Available at: http://kns.cnki.net/kcms/detail/51.1773.tb.20220525.0847.002.html.

Whiting, P. J., and Dietrich, W. E. (1993). Experimental studies of bed topography and flow patterns in large-amplitude meanders: 2. Mechanisms. *Water Resour. Res.* 29 (11), 3615–3622. doi:10.1029/93wr01756

Xu, D., and Bai, Y. (2013). Experimental study on the bed topography evolution in alluvial meandering rivers with various sinuousnesses. *J. Hydro-environment Res.* 7 (2), 92–102. doi:10.1016/j.jher.2012.06.003

Zen, S., Gurnell, A. M., Zolezzi, G., and Surian, N. (2017). Exploring the role of trees in the evolution of meander bends: The Tagliamento River, Italy[J]. *Water Resour. Res.* 53, 5943–5962. doi:10.1002/2017WR020561

Zhang, H. T., Dai, W. H., da Silva, A. M. F., and Tang, H. W. (2021). Numerical model for convective flow in meandering channels with various sinuosities. *J. Hydraul. Eng.* 147 (11), 04021042. doi:10.1061/(asce)hy.1943-7900.0001917

Zhang, J. Y., Chen, L., Liu, L., and Wang, Z. G. (2007). The best bend shape of the middle and lower reaches of the Hanjiang River [J]. *J. Wuhan Univ. Eng. Ed.* 40 (1), 37–41. doi:10.3969/j.issn.1671-8844.2007.01.008

Zhou, J. Y. (2015). *Improvement and application of prediction methods for flow structure and fluvial processes in meander channels*. Beijing, China: Tsinghua University.

Zhu, L. L., Xu, Q. X., and Xiong, M. (2017). Causes of convex erosion, depression and siltation in the Xiajingjiang sharp bend channel after impoundment of the Three Gorges Reservoir [J]. *Adv. water Sci.* 28 (02), 193–202.

Glossary

The following symbols are used in this article:

R_{em} model Reynolds number

h_m model water depth (cm)

d_{50} median particle size (mm)

d sediment size (mm)

u sediment incipient velocity (m/s)

h water depth in Sha Yuqing formula (cm)

H water depth in the fitting formula of flume test (cm)

e porosity (take the value as 0.4)

Q streamflow (m^3/s)

C_s sediment concentration (g/m^3)

g_b sediment transport rate per unit width (g/s)

W runoff volume (m3, W=Q*Δt)

W_s sediment discharge (t)

κ curvature (m^{-1})

ρ radius of curvature (m)

U velocity of flow (cm/s)

U_{vag} average velocity of cross section (cm/s)

z water depth of measuring point (cm)

x starting distance (m)

B measuring river width (m)

C_s sediment concentration (g/m^3)

C_{svcg} average sediment concentration of section (g/m^3)

γ_s sediment bulk density (g/cm^3)

γ water bulk density (g/cm^3)

α_L horizontal scale

α_H vertical scale

α_V velocity scale

α_n roughness scale

α_Q rate of flow scale

α_{t_1} time of flow scale

α_ω subsiding velocity scale

α_{γ_0} dry capacity scale

α_d particle size scale

α_s sediment concentration scale

α_{t_2} riverbed deformation time scale (riverbed deformation caused by suspended load movement)

α_{V_0} starting velocity scale

α_{q_b} bed load transport rate per unit width scale

α_{t_3} riverbed deformation time scale (riverbed deformation caused by bed load movement).